Transcriptomic analysis of perirhinal and lateral entorhinal cortex sub-regions in male mice

Beatriz B. Aoyama[1,2], Saul Lindo Samanamud[2,3], João P. D. Machado[1,2], André Schwambach Vieira[1,2]

1 Laboratory of Electrophysiology, Neurobiology and Behaviour, Dept. Functional and Structural Biology, Institute of Biology, University of Campinas, Campinas, São Paulo, Brazil

2 Brazilian Institute of Neuroscience and Neurotechnology (BRAINN), Campinas, São Paulo, Brazil

3. Department of Translational Medicine, School of Medical Sciences, University of Campinas, Campinas, São Paulo, Brazil

Correspondence to:
André Schwambach Vieira, Ph.D.
Department of Structural and Functional Biology
Institute of Biology
Rua Monteiro Lobato, 255 - Bloco J - 1 piso - Sl 16
Cidade Universitária "Zeferino Vaz"
University of Campinas – UNICAMP
Campinas - SP, Brazil, 13083-862
Phone: +55 19 35216197
Email:asv@unicamp.br

- **Abstract**

The perirhinal cortex (PER) is crucial for object recognition memory and is divided into areas 35 and 36, which have distinct cytoarchitectural and connections. The lateral entorhinal cortex (LEC), subdivided into dorsolateral (DLE) and ventral intermediate (VIE) regions, processes visual and spatial information, projecting it to the hippocampus. However, molecular studies that separately analyze these regions and their cellular populations are lacking, which hinders the identification of marker genes and the understanding of their molecular profiles. In this context, our study investigated the molecular profile of the aforementioned regions using male C57BL/6 mice whose samples were subjected to laser microdissection (LCM). Areas 35 and 36 of the PER and the DLE and VIE subregions of the LEC were isolated and submitted to RNA-seq analysis. Sequencing read alignment was performed using the STAR package, and statistical analysis was carried out with the DESeq2 package to estimate gene expression in the regions of interest. The results were divided into two parts. First, areas 35 and 36 of the PER were analyzed separately, revealing 1 differentially expressed gene between A35 and A36, 167 between A35 and DLE, 708 between A36 and DLE, 693 between VIE and DLE, 1,154 between A35 and VIE, and 1,591 between A36 and VIE. In the second part, areas 35 and 36 were considered as a single PER region, identifying 657 differentially expressed genes between PER and DLE and 1,878 between PER and VIE. Greater segregation of the transcriptomic profile was found between physically distant regions (areas 35 and 36 vs. VIE, DLE vs. VIE) compared to physically closer regions (A35 vs. A36; areas 35 and 36 vs. DLE). Additionally, our transcriptomic analysis identified potential marker genes for PER (6 genes more highly expressed in PER compared to LEC subregions), DLE (4 genes more highly expressed in DLE compared to PER and VIE), and VIE (8 genes more highly expressed in VIE compared to PER). In *silico* analysis showed shared enrichment of *neuroactive ligand receptor interaction pathway* in all comparisons, considering PER areas both separately and together. In the comparison between areas 35 and 36 with LEC, there was higher expression of genes encoding receptors of melanocortin, leptin, and glucagon, suggesting that PER, compared to LEC, would be more sensitive to these hormones and participate of nutritional status of the organism. There was also higher expression of genes associated with axonal guidance of glutamatergic neurons in DLE compared to VIE, which may be linked to an increased neuroplasticity mechanisms pro-excitability in the dorsal LEC region. Supporting this hypothesis, higher expression of the genes *BDNF*, *GDFN* α1 receptor were observed in DLE compared to VIE. Thus, our study is the first to show the molecular differences in areas 35 and 36 of the PER and the DLE and VIE subregions of the LEC. These findings may contribute to the understanding of these regions and the identification of specific molecular markers for cellular populations, helping to infer possible functional roles of these populations based on the molecular profile identified.

Keywords: Perirhinal cortex, Entorhinal cortex, Transcriptomics

1. Introduction

The perirhinal cortex (PER) is located dorsally to the temporal association cortex (TeA), caudally to the post-rhinal cortex (POR) and ventrally to the lateral entorhinal cortex (LEC) [1]. The PER is important for recognizing object's representations, it creates associations that allow tactile recognition[2,3] and it is composed of areas 35 and 36 (Fig. 1A). PER area 35 is considered an agranular cortex in view of its lack of VI layer[4,5]. This area is involved in cognitive processing and anatomically, area 35 is located dorsally to the area 36, ventrally to the entorhinal cortex, caudally to the POR and below the rhinal fissure in rostral levels. PER area 36 is considered dysgranular due to disorganized laminar structure[6], which is one of the main characteristics that differs it from the area 35 cytoarchitecture. Area 36 is anatomically located dorsally to the visceral cortex and somatosensory cortex, and is located ventrally to the auditory association cortex.

The lateral entorhinal cortex (LEC), a subdivision of the entorhinal cortex (EC), plays a key role in representing events, contexts, and their sequences[7-10]. This region is also crucial for processes related to memory and learning[11-14]. The LEC is subdivided into three bands, dorsolateral (DLE), dorsal intermediate (DIE) and ventral intermediate (VIE)[6] (Fig.1A). The DLE band is essential for representing ongoing experiences, especially associated with contextual information and temporal order[15]. The DLE band primarily projects to the septal and dorsal regions of the hippocampal formation, whereas the VIE band, situated in the ventral portion of the LEC, projects to the ventral hippocampal formation and the lateral perforant pathway[15].

The PER and the LEC are crucial for the hippocampal network (Fig.1B), acting as entry points for information to and from neocortical and subcortical structures, providing data on objects, motivation, and attention[9,16-18]. This integration of information between PER and LEC is essential for creating specific object-related contexts and contributes to episodic memory formation in the hippocampus[19-21]. Given the importance of PER and LEC in the hippocampal network, this study aimed to investigate, using laser microdissection and RNA-sequencing, the molecular profiles of the PER (areas 35 and 36) and LEC subregions (DLE and VIE), as well as to identify potential marker genes for these regions.

2. Methods

2.1 Animals

Three-month-old male mice (C57BL/6) were used in this study, 5 animals were used for RNA-sequencing and 3 animals were used for histological reference slides preparation. Animals were housed in a 12-h light/dark cycle on a ventilated rack with free access to food and water throughout the experimentation process. The experiments were performed at the University of Campinas and the experimental protocol was approved by University research ethics committee (CEUA 5682-1; 2020 protocol) according to accepted ethical practices and legislation regarding animal research in Brazil (Brazilian federal law 11.794 from October 8th, 2008).

2.2 Morphological identification of cortical areas of interest

The areas 35 and 36 of the PER, as well as the DLE and VIE subregions of the LEC, were defined based on The Allen Mouse Brain Atlas (portal.brain-map.org) and previously published studies[1,2]. The histological reference slides were produced in a Cryostat using fixed brains. Coronal serial sections of 45 µm were produced for each brain, mounted on glass slides and Nissl stained. The slices were classified into rostral, intermediate and caudal slices using the entire hippocampus as a guide structure and the lateral distance was used to measure the end of one region to the beginning of the next region.

Rostral slices were selected between the bregmas -1.82 and -2.80. Rostral slices included the granular layer of the dorsal dentate gyrus, external capsule, endopiriform nucleus and piriform cortex as reference structures **(Fig.1C, D,E)**. Area 36 was identified based on its lateral distance from area 35, as both form horizontal bands along the rostrocaudal axis, according to the 3D model from the Mouse Brain Atlas. In these sections, the lateral distance measured was 196-197 µm for areas 35 and 36 of the PER, and 288-289 µm for the DLE region. Intermediate slices were selected between the bregmas -2.92 and -3.64. The intermediate slices included the dorsal and ventral dentate gyrus, dorsal and ventral CA3, and post-piriform transitional area as reference structures (**Fig. 1F,G,H).** In these sections, the lateral distance measure was 196-197 µm for areas 35 and 36 of the PER and 400-401 µm for the DLE region.

Caudal sections were selected between bregma -3.80 and -4.04. These caudal sections included the same reference structures as the intermediate sections **(Fig.1I,J,K)**, however, for slices near bregma -4.04, we considered sections without the presence of CA3, but with both dorsal and ventral dentate gyrus, absence of the polymorphic layer, and presence of the medial band of the dorsal zone of the entorhinal cortex. In these sections, the lateral distance measure was 196-197 µm for areas 35 and 36 of the PER, 400-401 µm for the DLE subregion and 411-412 µm for the VIE subregion.

2.3 Laser Microdissection

The morphological identification parameters stated above were used to identify areas 35 and 36 of PER, and subregions DLE and VIE of LEC in frozen brains. For laser microdissection, previously frozen brains were sectioned using a cryostat (Leica Biosystems) to obtain 60 µm serial sections for RNA sequencing, with the entire hippocampus used as a reference structure. The coronal slices were collected in PEN membrane-covered slides (Life Technologies®, Thermo Fisher Scientific) and these slides were stained with Cresyl Violet, dehydrated with an ethanol series and stored at 80C. The structures were delimited using a PALM (Zeiss®) system and the tissue was mechanically collected in separate tubes using surgical microscope and ophthalmic forceps.

2.4 RNA isolation, cDNA library preparation and RNA sequencing

RNA was isolated from microdissected samples using Trizol's manufacturer protocol for RNA isolation (Thermo Fisher Scientific). Subsequently, cDNA libraries were produced using NEBNext Poly(A) mRNA Magnetic Isolation module for mRNA isolation and VAHTS Universal V8 RNA-seq Library Prep Kit for MGI kit following the manufacturer instructions.

Sequencing was performed in an Hiseq platform (Illumina) available from Macrogen Inc, producing an average of 22 million reads per sample. Reads were aligned to the *Mus musculus* genome GRCm38 Ensembl release 102 assembly using the STAR aligner tool. The alignment percentage was 83,14% and for the gene expression estimation and statistical analysis purposes, we use the The DESEq2 statistic package (http://www.bioconductor.org/packages/release/bioc/html/DESeq2.html).

A list of differentially expressed genes with a statistical significance of $p < .05$ (after correction for multiple tests) was generated. This list was submitted to enrichment analysis

using clusterProfiler package (https://bioconductor.org/packages/release/bioc/html/clusterProfiler.html, RRID:SCR_016884) (Yuet al., 2012) and the functional profiles were classified into KEGG Pathways.

The transcriptomic analyses were divided into two parts. The first analysis focused on identifying upregulated and downregulated genes, as well as enriched pathways, from comparisons between areas 35 and 36 of the PER and the subregions DLE and VIE of the LEC. The second analysis focused on identifying upregulated and downregulated genes, as well as enriched pathways, considering comparisons between PER (areas 35 and 36 as an unique region) and the subregions DLE and VIE of the LEC.

Moreover, in the second part of the analysis, we focused on identifying the most highly expressed genes in PER, DLE, and VIE, by comparing them against each other to identify potential marker genes for these regions. For marker genes exploration, we applied a cutoff of log2FoldChange > 1.5. An exception was made for the DLE subregion where a log2FoldChange > 0.5 was used, given the lower number of differentially expressed genes identified in this area.

2.5 Transcriptomic data cross-validation

The validation involved the selection of *in situ* hybridization (ISH) sections images available on the online platform of the Allen Mouse Brain Atlas (https://mouse.brain-map.org/). We employed the same identifying criteria used for laser microdissection fo PER, DLE, and VIE along the rostro-caudal axis in order to select ISH section images. The genes *MC4R, Lepr, Sema3E, Slc17a8, BDNF*, and *Gfra1* were analyzed, with an average of 17 sections per gene. Using the ImageJ software, the regions of interest were selected with the ROI Manager tool, and an average threshold (120-188.16) was established. The average percentage of the area was measured after applying the average threshold to the areas of interest, PER, LEC, DLE and VIE, in which we used the same methods to identify the regions described in the methodology. The average percentage of the area was measured considering rostral, intermediate, and caudal sections, as well as the separation of gene expression according to the rostro-caudal axis.

3. Results

The comparison between A36 vs A35 resulted in just one differentially expressed gene (gene *Ly86* up-regulated in A36 vs A35), which is the reason why this comparison was excluded from the following analysis. The comparison between A35 and DLE revealed 167 differentially expressed genes, in which 61 up-regulated genes and 105 down-regulated genes in A35 compared to DLE. The comparison between A36 and DLE, we found 708 differentially expressed genes, in which 292 up-regulated genes and 416 down-regulated genes in A36 compared to DLE. For the whole differentially expressed genes table, please refer to the Supplementary Table.

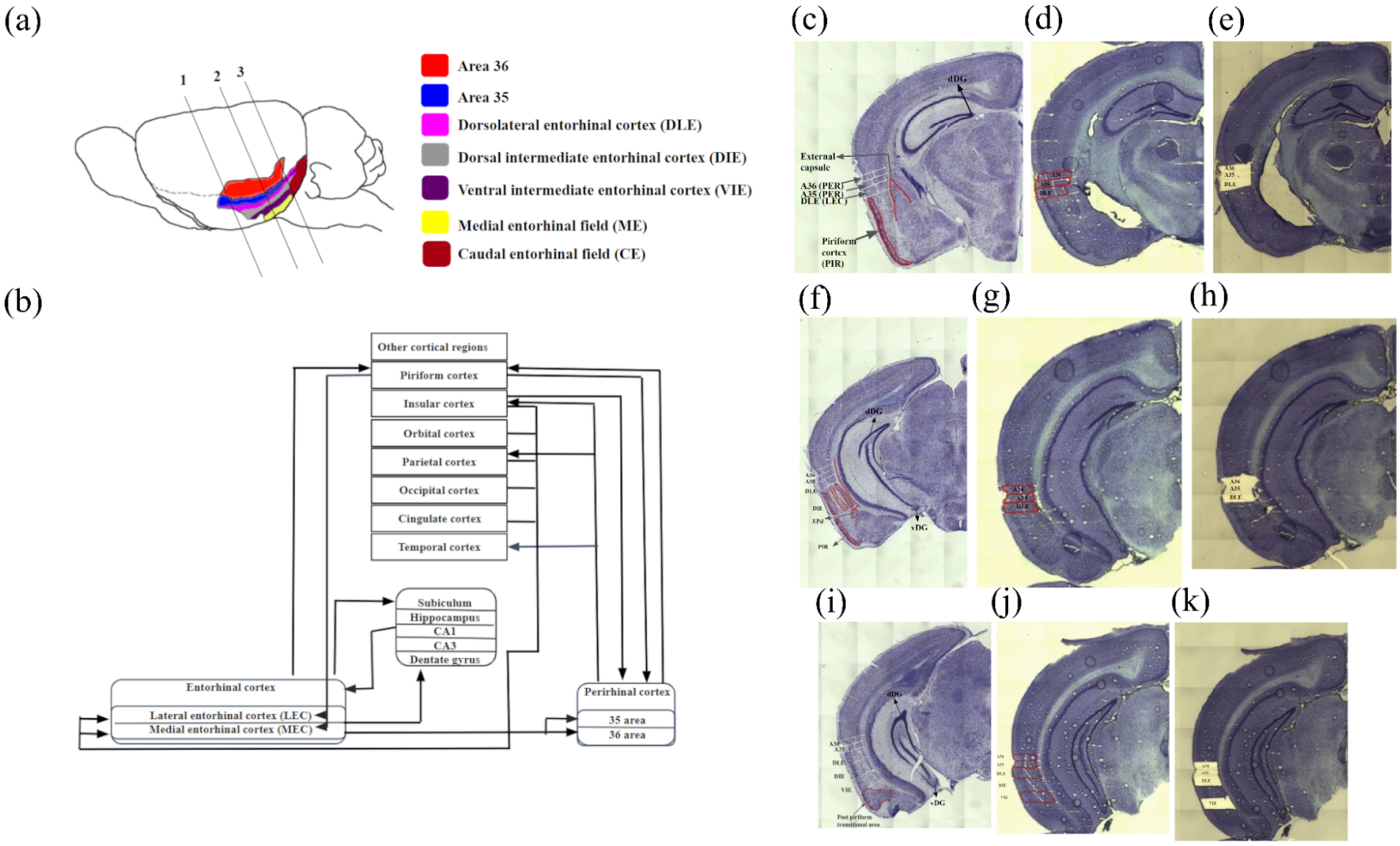
(a)
1
2
3
Area 36
Area 35
Dorsolateral entorhinal cortex (DLE)
Dorsal intermediate entorhinal cortex (DIE)
Ventral intermediate entorhinal cortex (VIE)
Medial entorhinal field (ME)
Caudal entorhinal field (CE)
(b)
Other cortical regions
Piriform cortex
Insular cortex
Orbital cortex
Parietal cortex
Occipital cortex
Cingulate cortex
Temporal cortex
Subiculum
Hippocampus
CA1
CA3
Dentate gyrus
Entorhinal cortex
Lateral entorhinal cortex (LEC)
Medial entorhinal cortex (MEC)
Perirhinal cortex
35 area
36 area
(c)
(d)
(e)
(f)
(g)
(h)
(i)
(j)
(k)
dDG
vDG
External capsule
A36 (PER)
A35 (PER)
DLE (LEC)
Piriform cortex (PIR)
A36
A35
DLE
DIE
EPd
PIR
VIE
Post piriform transitional area

Figure 1. (a) Adapted figure of mouse brain showing areas 35 (in blue) and 36 (in red) of perirhinal cortex (PER), subregion dorsolateral (DLE) in pink, dorsal-intermediate (DIE) in gray and ventral intermediate (VIE) in purple of lateral entorhinal cortex (LEC), subregion medial (ME) in yellow and caudal in brown of medial entorhinal cortex (MEC). (b). Figure showing the network between PER, lateral and medial entorhinal cortex, hippocampus and other cortical regions. (c),(f),(i) Figures showing coronal fixed mouse brain slices in the rostral, intermediate and caudal axis respectively. Structures as the dorsal (dGD) and ventral (vGD) dentate gyrus, external capsule, piriform cortex and post-piriform transitional area were used as reference to identify the areas 35/36 of PER and subregions of LEC. (d),(g),(j) Figures of coronal mouse brain slices showing the rostral, intermediate and caudal axes respectively with the PER, DLE and VIE selected in red before the LCM. (e),(h),(k) Figures of frozen mouse brain showing the rostral, intermediate and caudal axes respectively with the PER, DLE and VIE after LCM and removal of structures.

The comparison between A35 and VIE showed 1154 differentially expressed genes, in which 544 up-regulated genes and 610 down-regulated genes in A35 compared to VIE. The comparison between A36 and VIE identified 1591 differentially expressed genes, in which 723 up-regulated genes and 867 down-regulated genes in A36 compared to VIE. Finally, the comparison between DLE and VIE revealed 693 differentially expressed genes, in which 364 up-regulated genes and 693 down-regulated genes in DLE compared to VIE.

For the second transcriptomic analysis, we found 657 differentially expressed genes in PER compared to DLE, in which 248 up-regulated genes and 409 down-regulated genes in PER compared to DLE. In the comparison between PER and VIE, we observed a total of 1878 differentially expressed genes, in which 848 up-regulated genes and 1029 down-regulated genes. The complete list of differentially expressed genes is presented in the supplementary material.

The principal component analysis (PCA) clustered the samples according to their respective regions in both transcriptomic analyses (Fig. 2A, G), except in the first analysis (Fig. 2A), areas 35 and 36 of PER, clustered together. In the analysis for potential marker gene discovery, we investigated genes with a higher expression in a region as compared to the others, according to the logFoldChange criteria described in the methodology. We observed a total of 6 most expressed genes in PER compared to the LEC subregions, 8 most expressed genes in VIE compared to PER and DLE and 4 most expressed genes in DLE compared to PER and VIE.

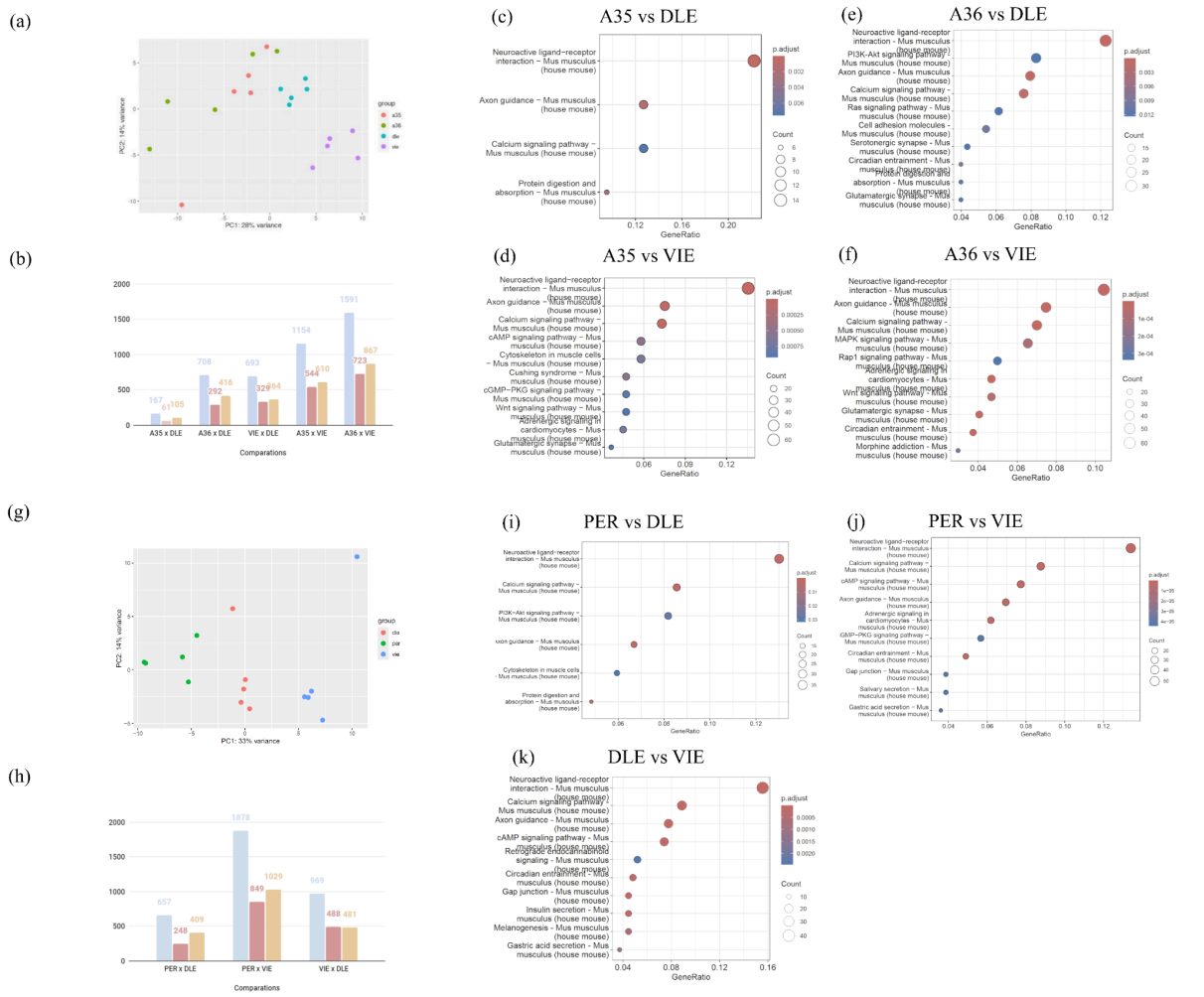

Figure 2. (a),(g) Figure showing the principal component analysis (PCA) considering the transcriptomic analysis 1 with A35 in orange, A36 in green, DLE in blue, VIE in purple. The PCA considered the transcriptomic analysis 2 with PER in green, DLE orange and VIE in blue. (b),(h) Graphics showing the total number of differentially expressed genes in blue, the up-regulated genes in red and the down-regulated genes in orange in transcriptomic analysis 1 and 2. (c),(d),(e),(f) Graphics of enrichment pathways based on differentially expressed genes in comparisons between A35 vs DLE, A35 vs VIE, A36 vs DLE and A36 vs VIE respectively, (i),(j),(k) Graphics of enrichment pathways based on on differentially expressed genes in comparisons between PER vs DLE, PER vs VIE and DLE vs VIE respectively.

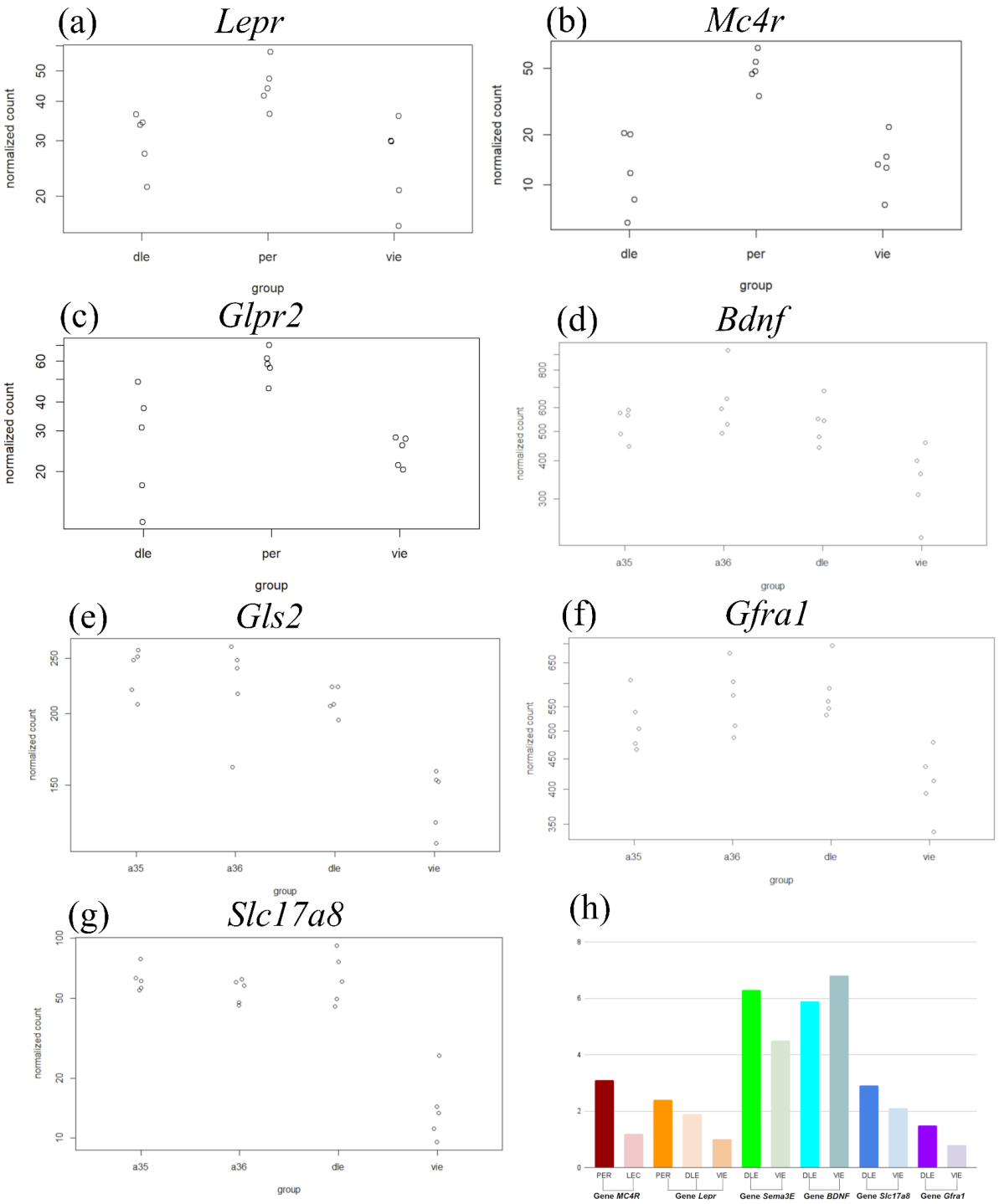

Figure 3. Graphics showing gene expression estimation based on RNA-seq for the genes *Lepr, Mc4r, Glpr2, Bdnf*, *Gls2, Gfra1*, and *Slc17a8*. The X-axis shows the groups A35, A36, DLE, and VIE for the genes *Bdnf*, *Gls2*, *Gfra1*, and *Slc17a8*, and the groups PER, DLE, and VIE for the genes *Lepr* and *Mc4r*. The Y-axis shows the normalized count for each gene. The last graph illustrates the validation using IHS for the expression of genes *Lepr* (orange), *Mc4r* (red), *Sema3E* (green), *Bdnf* (blue), *Gfra1* (purple), and *Slc17a8* (dark blue). The X-axis shows the area percentage counts, and the Y-axis shows the regions PER, LEC, DLE, and VIE. Darker colors indicate higher area percentages, while lighter colors indicate reduced area percentages. (a) Gene expression for *Lepr*. (b) Gene expression for *Mc4r*. (c) Gene expression for *Glpr2*. (d) Gene expression for *Bdnf*.

(e) Gene expression for *Gls2*. (f) Gene expression for *Gfra1*. (g) Gene expression for *Slc17a8*. (h) Area percentage per region according to the gene expression of IHS.

The most enriched pathways in both transcriptomic analysis considering differentially expressed genes were *neuroactive ligand receptor interaction*, *axon guidance* and *calcium signaling* **(Fig.2c-k)**. The complete list of enriched pathways in all comparisons are in the supplementary material. Moreover, we observed the most expression of *Lepr* (leptin receptor), *MC4R* (melanocortin 4 receptor) and *Glpr2* (glucagon-like peptide 2 receptor) genes in PER comparing to LEC (**Fig.3A,3B,3C)**; most expression of *BDNF* (brain-derived neurotrophic factor) **(Fig.3D)**, *Slc17a8* (vesicle glutamate transporter 3) **(Fig.3E)**, *GLS2* (glutaminase 2), *Gfra1* (GDNF Family Receptor Alpha 1) in DLE compared to VIE **(Fig. 3G).**

Regarding the validation, we selected the key genes from the most enriched pathways and explored ISH data from the online Allen Mouse Brain platform, for such genes. The genes *Lepr, MC4R, Sema3E, BDNF, Slc17a8*, and *Gfra1* (Fig. 3H) were selected for such validation. We measured the area percentage along the hippocampal rostro-caudal axis for the regions of interest (PER, LEC, DLE, and VIE) according to the genes of interest (supplementary material).

The ISH data showed an average of 3.1 for PER and 1.2 for LEC regarding the *MC4R* gene, this finding supports our hypothesis of higher gene expression in the PER compared to the LEC, and in the PER compared to the VIE.

Moreover, we observed that the highest expression of this gene by ISH was in intermediate and caudal sections in PER compared to the same in LEC, as described in the supplementary material. For the *Lepr* gene, our data showed an average area percentage of 1.4 for PER, 1.9 for DLE, and 1 for VIE. However, unlike the expression of the *MC4R* gene by ISH, the highest expression of the *Lepr* gene by ISH was present in rostral sections in PER and DLE.

In the validation of genes associated with axon guidance, synaptic neuroplasticity mechanisms, and glutamate transport in the comparison of DLE with VIE, we observed an average area percentage of 6.3 in DLE and 4.5 for VIE for the *Sema3E* gene, with this gene being more expressed by ISH in caudal sections in DLE, as described in the supplementary material. We observed higher expression of the *Slc17a8* and *Gfra1* genes by ISH in DLE (1.9

and 1.5, respectively) compared to VIE (2.1 and 0.8, respectively). However, regarding the *Slc17a8* gene, we observed that the highest expression of this gene by ISH occurred in intermediate and caudal sections in DLE, while for the *Gfra1* gene, the highest expression by ISH was concentrated in rostral sections in DLE. Regarding the *BDNF* gene, we observed an average area percentage of 6.8 in the VIE and 5.9 in the DLE.

4. Discussion

This study presents for the first time the transcriptomic profile of areas 35 and 36 of the PER and subregions of DLE and VIE of the LEC microdissected by LCM. The observed higher expression of genes that code for the receptors of melanocortin, glucagon and leptin in PER compared to LEC suggests that PER might be more sensitive to hormonal signaling involved in hunger/satiety, which could influence its function according to the organism's nutritional state. When comparing DLE to VIE, the higher expression of genes associated with axon orientation, neurotrophins, production and vesicular transport of glutamate indicates an enhanced neuroplasticity machinery in DLE.

4.1 Nutritional state sensitivity in PER vs LEC

Among the higher expressed genes in PER when compared to DLE and VIE we observe an enrichment of the *neuroactive ligand receptor interaction* pathway. We observed that the receptors expressed were associated to feeding, feed seeking and energetic state of the organism. Our results found up-regulation of *MC4R* no PER (A35 and A36) compared to LEC; *GLP2R* gene in PER (A35 e A36) compared to LEC; and *Lepr* gene in PER (A36) compared to VIE.

Leptin is a hormone produced by adipocytes that circulates throughout different regions including the brain. In the rodent brain, the leptin receptor can be expressed in the hypothalamus (arcuate nucleus), cortex, amygdala, hippocampus, brainstem and cerebellum [117]. Studies have demonstrated that the interaction between leptin and its receptor is important for weight control, feeding[117,118], nutritional state control [119,118,120] and cognitive function[241,242]. Our data showed the increased expression of *Lepr* gene in PER compared to VIE **(Fig 3A)**.

This finding was also observed in the IHS data from the online platform Mouse Allen Brain, especially in rostral slices where *Lepr* gene expression is significant in PER compared to other cortical regions. Therefore, our data suggests that the PER may be more sensitive to leptin hormone signaling than the VIE.

The MC4R receptor is found in different mouse brain regions such as hippocampus, cortex, medial prefrontal cortex (mPFC), brainstem, paraventricular nucleus, hypothalamus and spinal cord[121,122]. The melanocortin and MC4R interaction in hypothalamic nucleus [121] is important in controlling food seeking, feeding[123] and weight[124,125]. Studies have shown that MC4R gene is also found expressed in the arcuate nucleus[122,126] and it participates in the hypothalamus-leptin-melanocortin system in energic homeostasis regulation[122,127]. Our data found up-regulation of *MC4R* gene in PER compared to LEC **(Fig 3B)**. This finding could also be observed in the IHS data from online platform Mouse Allen Brain. Therefore, our data suggests that the PER may be more sensitive to melanocortin hormone signaling than the LEC.

Furthermore, we also found the up-regulation of the GLP2R gene in PER compared to LEC. The GLP2R receptor codifies the Glucagon-like peptide-2 receptor, which is widely expressed in arcuate nucleus, the compact region of the dorsomedial nucleus of the hypothalamus[131], brainstem[130,132], hippocampus and cortex in mice[129]. The Glucagon-like peptide-2 (GLP2) hormone binds to the GLP2R receptor, and this interaction controls feeding behavior. As a matter of fact, GLP2 functions as a neurotransmitter in the brainstem and hypothalamus synaptic transmission [132]. The GLP2R would be involved in neuroprotective and neuromodulatory functions [243] in energetic balance control [244]. Our data showed increased expression of GLP2R in PER compared to VIE (Fig.3C). Therefore, the up-regulation of this receptor in PER compared to LEC suggests that PER could have increased sensibility to the GLP-2 hormone than LEC.

Most studies focus on these receptors in the hypothalamus, a region well known for its central role in regulating appetite and food intake under various dietary conditions. However, the functional role of the PER in response to different dietary conditions remains unclear. Our data demonstrated that the PER may play a significant role in this context given the differential expression of leptin, melanocortin and peptide-like glucagon receptors compared to the LEC. This finding suggests that PER could be more responsive to the organism's nutritional state alterations, resulting in possible modulation of PER function depending on

nutritional status. A possibility would be that object recognition or object saliency on the environment could be impacted by a state such as hunger.

Moreover, in order to validate this data, we utilized IHS from the online platform Allen Mouse Brain, as described in the methodology. The IHS validation data showed that the average percentage of area for the MC4R and Lepr genes (Fig. 3H) supports our hypothesis of higher gene expression in the PER compared to the LEC, and in the PER compared to the VIE.

Our study also hypothesizes functional implications of our findings. We suggested that up-regulation of *Lepr, MC4R* and *GLPR-2* in PER compared to LEC, could also be associated with an evolutionary survival behavior linking memory to feeding, as shown by the literature review conducted by Seitz and collaborators (2021) [140]. The authors hypothesized that the activation of episodic memory would be associated with feeding behavior, enhancing learning in the search for food as a form of survival, potentially influencing future food intake [141].

Information about food and/or feeding behavior, such as the recognition of food (whether they are food or not), places where this food might be found, distinctions between different types of food (palatable or aversive), and familiarity with these foods, would involve the activation of the memory circuit associated with exploration and locomotion for survival in different environments.

One of the main PER functions is to recognize multimodal representations associated with objects, and maybe, in these contexts, the objects could be food and are considered objects. Thus we could find differential gene expression of receptors associated with the organism's nutritional state.

Therefore, our findings are the first to indicate that the PER, in relation to the LEC, may be more sensitive to the hormonal signaling of leptin, melanocortin, and glucagon-like peptide. These findings suggest (1) that changes in the organism's nutritional state could influence PER function, and (2) that possible functional implications may be associated with a survival behavior in the animal, activating memory and learning circuits in the search for and ingestion of food. However, functional studies need to be conducted to confirm these hypotheses.

4.2 Axon guidance and neuroplasticity genes in DLE vs VIE

Our data also showed up-regulation of genes associated with axon guidance in DLE compared to VIE. The axon guidance is a dynamic process, in which guidance receptors are expressed in growing ends of motile axons and it interacts with signaling molecules or membrane-anchored molecules, resulting in the attraction, repulsion, or growth of axonal extensions[142]. This guidance process is important for remodeling, maintenance and organizing mature synapses[143]. Our results showed the up-regulation of *Sema7a* (semaphorin 7A), *Sema3e* (semaphorin 3E), *Epha7* (receptor EphA7) e *Efna5* (Ephrin A5) in DLE compared to VIE

Semaphorin 3E is part of the semaphorin class 3 family. The Sema3E binds to neuropilin and plexin receptors[158], this interaction is important for mediating repulsive signals in dorsal root ganglion neurons[159] and retinal ganglion neurons[160]. According to the Watakabe and colleagues (2006) study[145,161], the authors observed mRNA Sema3E expression in GABAergic interneurons in deep layers Vb and VI of primary motor area, secondary and primary somatosensory area and primary visual area in mice. These findings suggest that sema3E and its receptor plexin D1 interaction may result in repulsive actions that could contribute to the formation and maintenance of laminar-specific synaptic connectivity in the neocortex of mice. Although our data did not observe differential expression of *Plxnc1* in DLE compared to VIE, the up-regulation of *Sema3E* in DLE, compared to VIE, suggests a higher inhibition of inhibitory synapses growth in DLE as compared to VIE.

Semaphorin 7A usually binds to plexin 1C[162,163] and participates in synapse development and neuroglia plasticity[164,165]. However, in adult neurons of mice, the sema7A interacts with integrin receptor β1, this interaction is important to promote dendritic growth in mature granule neurons in dentate gyrus[166]. Our data did not find differential expression in integrin receptor β1 gene in DLE compared to VIE, but the up-regulation of *sema7A* gene in DLE, compared to VIE, may indicate the possibility for more excitatory synapses growth in DLE as compared to VIE.

Ephrin-A5 is expressed in adult mice cortex, including the entorhinal cortex, mainly in layers 2,3 5[169], as well as granular neurons of the dentate gyrus[170]. In granular neurons of the dentate gyrus, the knockdown of the *Efna5* gene compromises the maintenance and proliferation of newly formed granular neurons. Thus, the up-regulation of *Efna5* gene in

DLE, compared to VIE, may be mediating more excitatory synapses growth in DLE as compared to VIE. Our data also found the up-regulation of the *Epha7* gene in DLE compared to VIE. The EphA7 binds to ephrin-A, particularly to the ephrin-A5, which has higher affinity [171, 172].

In the study performed by Clifford and colleagues (2014)[173], the authors observed that when deleting the *EphA7* gene (EphA7−/−) in developing cortical neurons and exposing them to ephrin-A5 surface *in vitro*, these neurons showed decreased repulsion compared to wild-type neurons, indicating that the EphA7 receptor, by interacting with ephrin-A5, may play a role in dendritic repulsion in cortical neurons. Moreover, the authors observed that this gene deletion also resulted in dendritic spine and filopodia growth during postnatal development, and reduction of excitatory synapses compared to WT neurons. Therefore, our data suggests the up-regulation of *Efna5* and *EphA7* genes in DLE, compared to VIE, could result in more excitatory synapses growth in DLE than in VIE.

Our data showing up-regulation of *Sema7A*, *Efrina A5* and *EphA7* in DLE, compared to VIE, could indicate more growth of excitatory synapses in DLE than in VIE. In contrast the up-regulation of Sema3E in DLE, compared to VIE, could be associated with inhibitory synapses growth repulsive actions in this region. Therefore, these findings suggest that DLE may have increased neuroplasticity mechanisms involved in excitability, when compared to VIE. Supporting this hypothesis, we observed an up-regulation of genes associated to neuroplasticity mechanisms which could be favoring excitatory synapses, such as BDNF (brain-derived neurotrophic factor) (Fig. 3D), GFRA1 (alpha-1 subunit of the glial cell line-derived neurotrophic factor receptor) (Fig. 3F), GLS2 (glutaminase 2) (Fig. 3E), and Slc17a8 (vGLUT3) (Fig. 3G), all more expressed in DLE when compared to VIE.

Neurotrophic factors are proteins that participate in maintenance and function of the nervous system in adult brain [185]. One of most important neurotrophic factors is BDNF (brain-derived neurotrophic factor), a factor widely expressed in both excitatory and inhibitory synapses, having a dependent activity related to synaptic plasticity [186,187]. BDNF and other neurotrophins are synthesized in the endoplasmic reticulum as pre-pro-neurotrophins. Pre-proBDNF is then converted into proBDNF through the removal of the signal peptide and subsequently cleaved to generate the mature form of BDNF [188], which is one of the markers of synaptic plasticity

Studies have been showing that BDNF and kinase tyrosine (TrkB) receptor are widely expressed in hippocampus and entorhinal cortex in rats [189,190], this interaction is important in synaptic plasticity mechanism in learning [189,190], memory recognition, and spatial memory [191,192,193,194,195]. The activation of TrkB by BDNF stimulates exocytosis of synaptic vesicles containing glutamate at presynaptic sites by activation of voltage-gated calcium channels (VGCC) [188].

Although our data did not reveal differential expression of genes associated with VGCC, our data may suggest that the up-regulation of BDNF in DLE, compared to VIE, could result in a greater role of this neurotrophic factor in DLE as compared to VIE. Supporting this hypothesis, we also observed the up-regulation of *GLS2* and *Slc17a8* genes in DLE compared to VIE, genes involved in glutamate synthesis and vesicular transport to the synaptic cleft. Therefore, our findings suggest a larger machinery involved in glutamate production, transport into synaptic vesicles, and release in a BDNF-dependent manner in DLE, compared to VIE. However, further experiments are required to confirm this observations regarding the *BDNF* gene in DLE.

The GFRα proteins are receptors for glial cell line-derived neurotrophic factors (GDNF). These receptors bind into GFLs (GDNF ligand family), which are part of the transforming growth factor-β (TGF-β) superfamily [196]. The receptor GRFα1 is expressed in the cortex, olfactory areas and hippocampus formation [198], as shown by recent IHS data available on the Allen Brain online platform. Studies have been showing that GDNF contributes to synaptic plasticity by stimulating the neurotransmitter releasing in synaptic terminals, which increases the AMPA receptors activity, such as GluR2 subunits. It plays an important role in synaptogenesis, neuronal network formation [199,196] and synaptic organization in hippocampal neurons [200]. The study performed by Irala et al. (2016) [200] demonstrated the interaction between GFRα1 and GDNF would be important in dendritic spines and dendrites development in hippocampal neurons in vivo and in vitro.

Therefore, this interaction could be associated with excitatory synapses growth as a synaptic plasticity mechanism in the hippocampus. Although our data did not find a differential expression of the GDNF gene, we observed an increased expression of *GFRα1* gene in DLE, compared to VIE. This finding could indicate an increased response to GDNF in DLE, compared to VIE, which could potentially contribute to the enhancement of

excitatory synapses in this area. This hypothesis is aligned to the previous findings about axon orientation and glutamate production and vesicular transport in DLE compared to VIE.

The entorhinal cortex participates in synaptic plasticity by different LTP and LTD mechanisms, mediating information between hippocampus and other cortical regions[245]. However, no studies in the literature explore neuroplasticity mechanisms along the rostrocaudal axis in the lateral entorhinal cortex, making our study the first to explore this possibility. Most studies suggest that synaptic plasticity along the rostroventral axis of the hippocampus, mediated by LTP, is more intense at the dorsal pole compared to the ventral pole[179,180–182], mainly in Schaffer collaterals and CA1 synapses[178,183], while LTD appears to be equivalent at both the dorsal and ventral poles[178,183].

Thus, our RNA-seq results indicate that the DLE subregion, possibly due to its projections to the dorsal hippocampus, exhibits more pro-excitability neuroplasticity mechanisms than the VIE subregion. Our study performed an exploratory analysis to understand the molecular differences between the DLE and VIE. However, there is a lack of functional studies that separate the lateral entorhinal cortex into DLE and VIE. Among the few studies found, we highlight the research performed by Wilson and collaborators, 2013 [201]. The researchers measured neuronal activity using *c-fos* in different subregions of the LEC in rats during the context-object recognition (OCR) protocol to evaluate the animals' ability to recognize objects based on their contextual characteristics. The authors observed neuronal activity in the VIE and DIE, but not in the DLE, in animals performing the OCR task. However, extensive lesions in the VIE and DIE, and minor lesions in the DLE, compromise this task. Thus, the authors suggested that the VIE and DIE, due to their connections with the ventral hippocampus, are necessary for the execution of OCR, as this region is associated with the processing of non-spatial information [202203], and may be less critical for the formation of memory and spatial learning compared to the dorsal hippocampus [203,20433,205].

Although our study did not perform functional experiments, our data suggest that the more intense pro-excitatory neuroplasticity mechanisms in the DLE could be associated with spatial learning and memory formation related to exploration and navigation, since most DLE projections are to the dorsal hippocampus. On the other hand, the VIE, possibly due to less intense pro-excitatory neuroplasticity mechanisms and perhaps pro-inhibitory neuroplasticity mechanisms, compared to the DLE, would be more associated with the processing of

contextual information involving emotional circuits, as it primarily projects to the ventral hippocampus.

4.3 Validation

To validate this data, we utilized IHS data from the online platform Allen Mouse Brain for the genes *Lepr, MC4R, Sema3E, BDNF, Slc17a8*, and *Gfra1* (Fig. 3H) as described in the methodology. Although our study did not separate the regions of interest into rostral, intermediate, and caudal sections, and collected samples along the rostro-caudal axis, it is possible that the higher gene expression observed in the RNA-seq data could originate from intermediate and caudal sections for the *MC4R, Sema3E* and *Slc17a8* genes, and from rostral sections for the *Lepr* and *Gfra1* genes, as observed in the IHS data. Furthermore, when analyzing the data along the rostro-caudal axis for the expression of BDNF in the DLE region, we noticed that the intermediate and caudal sections show a higher average area percentage compared to the rostral sections in the same region, as described in the supplementary material. In some sections, the area percentage was higher and deviated from the pattern observed in other sections, particularly in the caudal sections VIE caudal sections, this could be explained by a possible expression saturation for this gene.

4.4 Marker genes in PER, DLE and VIE

In order to identify potentially marker genes in PER, DLE and VIE, we searched for genes whose expression was based on Log2Foldchange criteria described in the methodology. Similar methodologies were used in our lab to search for marker genes in the hippocampus formation. The study performed by Machado e colaboradores (2022) [112] observed the differential expression between the hippocampus subregions. In the present study, among the most expressed genes in PER, we found GRP (gastrin-releasing peptide receptor), MC4R (melanocortin 4 receptor), KL (klotho), and PRLR (prolactin receptor) were identified in the in situ hybridization (ISH) database from the Allen Brain Mouse Atlas, as described in the supplementary materials. Regarding the DLE subregion, only the genes Nrn1 (Neuritin 1) and Nefm (Neurofilament, medium polypeptide) were found in the in situ hybridization (ISH) database from the online Allen Brain Mouse platform, as described in the supplementary materials. Finally, in the VIE, only the genes Brs3 (Bombesin receptor subtype-3), Wnt2b (Wingless-Type MMTV Integration Site Family, Member 2B), and Hc (hemolytic complement) were found in the ISH database from the Allen Brain Mouse platform.

5. Conclusion

Our findings suggest that the PER may have a higher sensitivity to signaling from hormones involved in hunger/satiety as compared to DLE and VIE, potentially adjusting its function in response to the organism's nutritional state. Furthermore, our data suggests that DLE, when compared to VIE, may have a more pro-excitability neuroplasticity mechanism, as indicated by differential expression of axon guidance genes, and a larger machinery involved in glutamate production, transport into synaptic vesicles, and release in a BDNF-dependent manner.

6. References

1. Harvey, J. Leptin regulation of neuronal excitability and cognitive function. *Curr. Opin. Pharmacol.* **7**, 643–647 (2007).
2. Friedman, J. The long road to leptin. *J. Clin. Invest.* **126**, 4727–4734 (2016).
3. Meek, T. H. & Morton, G. J. Leptin, diabetes, and the brain. *Indian J. Endocrinol. Metab.* **16**, S534–42 (2012).
4. Lee, Y.-H., Magkos, F., Mantzoros, C. S. & Kang, E. S. Effects of leptin and adiponectin on pancreatic β-cell function. *Metabolism* **60**, 1664–1672 (2011).
5. Yin, H. *et al.* Low Plasma Leptin and High Soluble Leptin Receptor Levels Are Associated With Mild Cognitive Impairment in Type 2 Diabetic Patients. *Front. Aging Neurosci.* **10**, 132 (2018).
6. Forny-Germano, L., De Felice, F. G. & Vieira, M. N. do N. The Role of Leptin and Adiponectin in Obesity-Associated Cognitive Decline and Alzheimer's Disease. *Front. Neurosci.* **12**, 1027 (2018).
7. Li, X. *et al.* Melanocortin 4 receptor-mediated effects of amylin on thermogenesis and regulation of food intake. *Diabetes. Metab. Res. Rev.* **35**, e3149 (2019).
8. Wang, K. *et al.* Neuroanatomy of melanocortin-4 receptor pathway in the mouse brain. *Open Life Sci* **15**, 580–587 (2020).
9. de Souza Cordeiro, L. M. *et al.* Hypothalamic MC4R regulates glucose homeostasis through adrenaline-mediated control of glucose reabsorption via renal GLUT2 in mice. *Diabetologia* **64**, 181–194 (2021).
10. Tao, Y.-X. The Melanocortin-4 Receptor: Physiology, Pharmacology, and Pathophysiology. *Endocr. Rev.* **31**, 506–543 (2010).
11. Delhanty, P. J. D. *et al.* Functional characterization of a new human melanocortin-4 receptor homozygous mutation (N72K) that is associated with early-onset obesity. *Mol. Biol. Rep.* **41**, 7967–7972 (2014).
12. Cui, H. *et al.* Neuroanatomy of melanocortin-4 receptor pathway in the lateral hypothalamic area. *J. Comp. Neurol.* **520**, 4168–4183 (2012).
13. Raskiliene, A., Smalinskiene, A., Kriaucioniene, V., Lesauskaite, V. & Petkeviciene, J. Associations of , and Polymorphisms with Obesity-Related Parameters in Childhood and Adulthood. *Genes* **12**, (2021).
14. Guan, X. *et al.* GLP-2 receptor in POMC neurons suppresses feeding behavior and gastric motility. *Am. J. Physiol. Endocrinol. Metab.* **303**, E853–64 (2012).
15. Yusta, B. *et al.* Enteroendocrine localization of GLP-2 receptor expression in humans and rodents. *Gastroenterology* **119**, 744–755 (2000).
16. Tang-Christensen, M., Larsen, P. J., Thulesen, J., Rømer, J. & Vrang, N. The proglucagon-derived peptide, glucagon-like peptide-2, is a neurotransmitter involved in the regulation of food intake. *Nat. Med.* **6**, 802–807 (2000).
17. Lovshin, J., Estall, J., Yusta, B., Brown, T. J. & Drucker, D. J. Glucagon-like peptide (GLP)-2 action in the murine central nervous system is enhanced by elimination of GLP-1 receptor signaling. *J. Biol. Chem.* **276**, 21489–21499 (2001).
18. Amato, A. & Mulè, F. Protective potential of glucagon like peptide 2 (GLP-2) against the

neurodegeneration. *Neural Regeneration Res.* **14**, 1901–1902 (2019).

19. Guan, X. The CNS glucagon-like peptide-2 receptor in the control of energy balance and glucose homeostasis. *Am. J. Physiol. Regul. Integr. Comp. Physiol.* **307**, R585–96 (2014).
20. DeFalco, J. *et al.* Virus-assisted mapping of neural inputs to a feeding center in the hypothalamus. *Science* **291**, 2608–2613 (2001).
21. Seitz, B. M., Tomiyama, A. J. & Blaisdell, A. P. Eating behavior as a new frontier in memory research. *Neurosci Biobehav Rev* **127**, 795–807 (2021).
22. Higgs, S. & Spetter, M. S. Cognitive Control of Eating: the Role of Memory in Appetite and Weight Gain. *Curr Obes Rep* **7**, 50–59 (2018).
23. Accogli, A., Addour-Boudrahem, N. & Srour, M. Neurogenesis, neuronal migration, and axon guidance. *Handb. Clin. Neurol.* **173**, 25–42 (2020).
24. Yuasa-Kawada, J., Kinoshita-Kawada, M., Tsuboi, Y. & Wu, J. Y. Neuronal guidance genes in health and diseases. *Protein Cell* **14**, 238–261 (2023).
25. Takahashi, T. *et al.* Plexin-neuropilin-1 complexes form functional semaphorin-3A receptors. *Cell* **99**, 59–69 (1999).
26. Miyazaki, N. *et al.* Developmental localization of semaphorin H messenger RNA acting as a collapsing factor on sensory axons in the mouse brain. *Neuroscience* **93**, 401–408 (1999).
27. Steinbach, K., Volkmer, H. & Schlosshauer, B. Semaphorin 3E/collapsin-5 inhibits growing retinal axons. *Exp. Cell Res.* **279**, 52–61 (2002).
28. Polleux, F., Morrow, T. & Ghosh, A. Semaphorin 3A is a chemoattractant for cortical apical dendrites. *Nature* **404**, 567–573 (2000).
29. Watakabe, A., Ohsawa, S., Hashikawa, T. & Yamamori, T. Binding and complementary expression patterns of semaphorin 3E and plexin D1 in the mature neocortices of mice and monkeys. *J. Comp. Neurol.* **499**, 258–273 (2006).
30. Tamagnone, L. *et al.* Plexins are a large family of receptors for transmembrane, secreted, and GPI-anchored semaphorins in vertebrates. *Cell* **99**, 71–80 (1999).
31. Liu, H. *et al.* Structural basis of semaphorin-plexin recognition and viral mimicry from Sema7A and A39R complexes with PlexinC1. *Cell* **142**, 749–761 (2010).
32. Uesaka, N. *et al.* Retrograde semaphorin signaling regulates synapse elimination in the developing mouse brain. *Science* **344**, 1020–1023 (2014).
33. Parkash, J. *et al.* Semaphorin7A regulates neuroglial plasticity in the adult hypothalamic median eminence. *Nat. Commun.* **6**, 6385 (2015).
34. Jongbloets, B. C. *et al.* Stage-specific functions of Semaphorin7A during adult hippocampal neurogenesis rely on distinct receptors. *Nat. Commun.* **8**, 14666 (2017).
35. Cooper, M. A., Crockett, D. P., Nowakowski, R. S., Gale, N. W. & Zhou, R. Distribution of EphA5 receptor protein in the developing and adult mouse nervous system. *J. Comp. Neurol.* **514**, 310–328 (2009).
36. Hara, Y., Nomura, T., Yoshizaki, K., Frisén, J. & Osumi, N. Impaired hippocampal neurogenesis and vascular formation in ephrin-A5-deficient mice. *Stem Cells* **28**, 974–983 (2010).
37. Gale, N. W. *et al.* Eph receptors and ligands comprise two major specificity subclasses and are reciprocally compartmentalized during embryogenesis. *Neuron* **17**, 9–19 (1996).

38. Himanen, J.-P. *et al.* Repelling class discrimination: ephrin-A5 binds to and activates EphB2 receptor signaling. *Nat. Neurosci.* **7**, 501–509 (2004).
39. Clifford, M. A. *et al.* EphA7 signaling guides cortical dendritic development and spine maturation. *Proc. Natl. Acad. Sci. U. S. A.* **111**, 4994–4999 (2014).
40. Huang, E. J. & Reichardt, L. F. Neurotrophins: roles in neuronal development and function. *Annu. Rev. Neurosci.* **24**, 677–736 (2001).
41. Tyler, W. J., Perrett, S. P. & Pozzo-Miller, L. D. The role of neurotrophins in neurotransmitter release. *Neuroscientist* **8**, 524–531 (2002).
42. Wardle, R. A. & Poo, M.-M. Brain-derived neurotrophic factor modulation of GABAergic synapses by postsynaptic regulation of chloride transport. *J. Neurosci.* **23**, 8722–8732 (2003).
43. Leal, G., Bramham, C. R. & Duarte, C. B. Chapter Eight - BDNF and Hippocampal Synaptic Plasticity. in *Vitamins and Hormones* (ed. Litwack, G.) vol. 104 153–195 (Academic Press, 2017).
44. Yan, Q. *et al.* Immunocytochemical localization of TrkB in the central nervous system of the adult rat. *J. Comp. Neurol.* **378**, 135–157 (1997).
45. Kaplan, D. R. & Miller, F. D. Neurotrophin signal transduction in the nervous system. *Curr. Opin. Neurobiol.* **10**, 381–391 (2000).
46. Kesslak, J. P., So, V., Choi, J., Cotman, C. W. & Gomez-Pinilla, F. Learning upregulates brain-derived neurotrophic factor messenger ribonucleic acid: a mechanism to facilitate encoding and circuit maintenance? *Behav. Neurosci.* **112**, 1012–1019 (1998).
47. Mizuno, M., Yamada, K., Olariu, A., Nawa, H. & Nabeshima, T. Involvement of brain-derived neurotrophic factor in spatial memory formation and maintenance in a radial arm maze test in rats. *J. Neurosci.* **20**, 7116–7121 (2000).
48. Cirulli, F., Berry, A., Chiarotti, F. & Alleva, E. Intrahippocampal administration of BDNF in adult rats affects short-term behavioral plasticity in the Morris water maze and performance in the elevated plus-maze. *Hippocampus* **14**, 802–807 (2004).
49. Bekinschtein, P. *et al.* Persistence of long-term memory storage requires a late protein synthesis- and BDNF- dependent phase in the hippocampus. *Neuron* **53**, 261–277 (2007).
50. Heldt, S. A., Stanek, L., Chhatwal, J. P. & Ressler, K. J. Hippocampus-specific deletion of BDNF in adult mice impairs spatial memory and extinction of aversive memories. *Mol. Psychiatry* **12**, 656–670 (2007).
51. Airaksinen, M. S. & Saarma, M. The GDNF family: signalling, biological functions and therapeutic value. *Nat. Rev. Neurosci.* **3**, 383–394 (2002).
52. Trupp, M., Belluardo, N., Funakoshi, H. & Ibáñez, C. F. Complementary and overlapping expression of glial cell line-derived neurotrophic factor (GDNF), c-ret proto-oncogene, and GDNF receptor-alpha indicates multiple mechanisms of trophic actions in the adult rat CNS. *J. Neurosci.* **17**, 3554–3567 (1997).
53. Shishkina, T. V. *et al.* Glial cell line-derived neurotrophic factor (GDNF) counteracts hypoxic damage to hippocampal neural network function in vitro. *Brain Res.* **1678**, 310–321 (2018).
54. Irala, D. *et al.* The GDNF-GFRα1 complex promotes the development of hippocampal dendritic arbors and spines via NCAM. *Development* **143**, 4224–4235 (2016).
55. Buzsáki, G. Two-stage model of memory trace formation: A role for 'noisy' brain states. *Neuroscience* **31**, 551–570 (1989).

56. Maggio, N. & Segal, M. Unique regulation of long term potentiation in the rat ventral hippocampus. *Hippocampus* **17**, 10–25 (2007).
57. Maggio, N., Shavit Stein, E. & Segal, M. Ischemic LTP: NMDA-dependency and dorso/ventral distribution within the hippocampus. *Hippocampus* **25**, 1465–1471 (2015).
58. Maruki, K., Izaki, Y., Nomura, M. & Yamauchi, T. Differences in paired-pulse facilitation and long-term potentiation between dorsal and ventral CA1 regions in anesthetized rats. *Hippocampus* **11**, 655–661 (2001).
59. Papatheodoropoulos, C. & Kostopoulos, G. Decreased ability of rat temporal hippocampal CA1 region to produce long-term potentiation. *Neurosci. Lett.* **279**, 177–180 (2000).
60. Canto, C. B., Wouterlood, F. G. & Witter, M. P. What does the anatomical organization of the entorhinal cortex tell us? *Neural Plast.* **2008**, 381243 (2008).
61. Dubovyk, V. & Manahan-Vaughan, D. Less means more: The magnitude of synaptic plasticity along the hippocampal dorso-ventral axis is inversely related to the expression levels of plasticity-related neurotransmitter receptors. *Hippocampus* **28**, 136–150 (2018).
62. Wilson, D. I. G. *et al.* Lateral entorhinal cortex is critical for novel object-context recognition. *Hippocampus* **23**, 352–366 (2013).
63. Bannerman, D. M. *et al.* Double dissociation of function within the hippocampus: spatial memory and hyponeophagia. *Behav Neurosci* **116**, 884–901 (2002).
64. Kjelstrup, K. G. *et al.* Reduced fear expression after lesions of the ventral hippocampus. *Proc Natl Acad Sci U S A* **99**, 10825–10830 (2002).
65. de Hoz, L., Knox, J. & Morris, R. G. M. Longitudinal axis of the hippocampus: both septal and temporal poles of the hippocampus support water maze spatial learning depending on the training protocol. *Hippocampus* **13**, 587–603 (2003).
66. Moser, E., Moser, M. B. & Andersen, P. Spatial learning impairment parallels the magnitude of dorsal hippocampal lesions, but is hardly present following ventral lesions. *J. Neurosci.* **13**, 3916–3925 (1993).
67. Moser, M. B. & Moser, E. I. Distributed encoding and retrieval of spatial memory in the hippocampus. *J Neurosci* **18**, 7535–7542 (1998).
68. Machado, J. P. D., Athie, M. C. P., Matos, A. H. B., Lopes-Cendes, I. & Vieira, A. S. The transcriptome of rat hippocampal subfields. Preprint at https://doi.org/10.1101/2021.06.23.449669.